Science Advances
AAAS

advances.sciencemag.org/cgi/content/full/5/1/eaau7447/DC1

Supplementary Materials for

Full in vivo characterization of carbonate chemistry at the site of calcification in corals

Duygu S. Sevilgen*, Alexander A. Venn, Marian Y. Hu, Eric Tambutté, Dirk de Beer, Víctor Planas-Bielsa, Sylvie Tambutté*

*Corresponding author. Email: stambutte@centrescientifique.mc (S.T.); sevilgen@centrescientifique.mc (D.S.S.)

Published 16 January 2019, *Sci. Adv.* **5**, eaau7447 (2019)
DOI: 10.1126/sciadv.aau7447

This PDF file includes:

Fig. S1. Simultaneous measurement of pH and carbonate by two LIX microsensors in the same location (distance between sensor tips, <10 μm) of the ECM within the growing edge of a *S. pistillata* microcolony.
Fig. S2. pH profiles measured in the polyps of different microcolonies of *S. pistillata* by entering a pH LIX microsensor through the polyp mouth (≈0 μm).
Fig. S3. Carbonate depth profile measured by entering a CO_3^{2-} LIX microsensor through the polyp mouth (at ~200 μm) of a *S. pistillata* microcolony.
Fig. S4. Retraction of the coral polyp upon microsensor insertion.
Note S1. Derivation of Eq. 1 to calculate DIC.
Note S2. Calculation of the compound SD for DIC and $\Omega_{arag.}$

Supplementary Materials

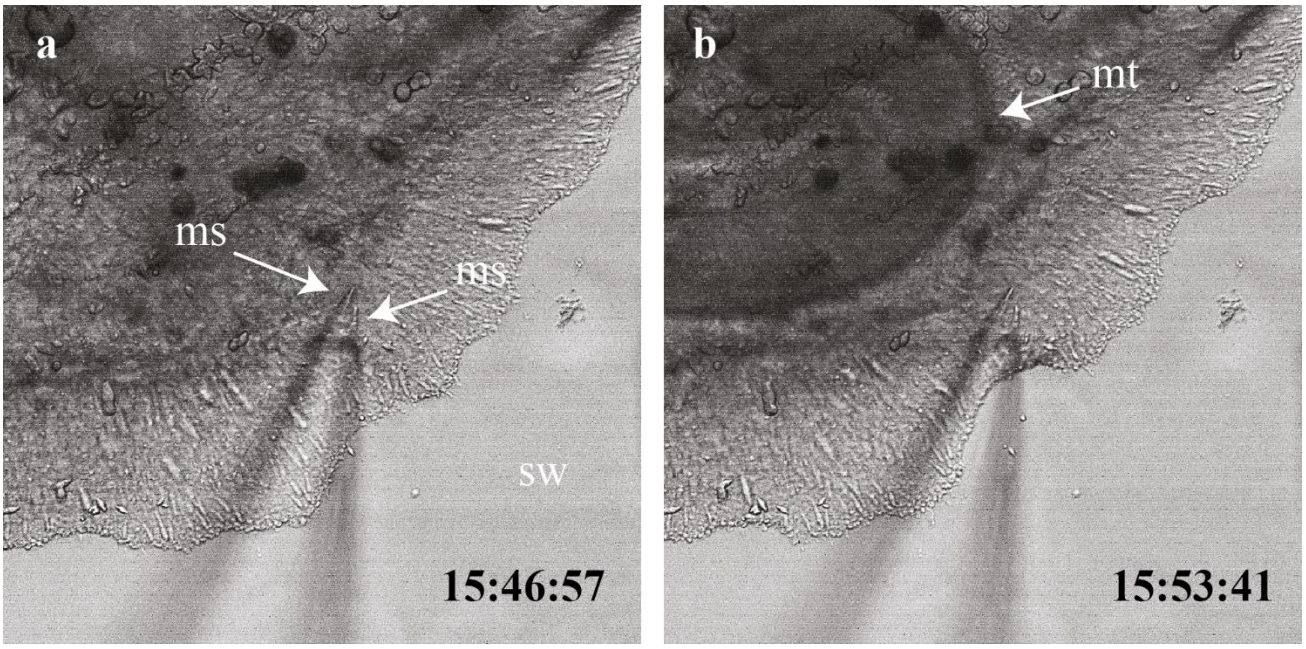

Fig. S1. Simultaneous measurement of pH and carbonate by two LIX microsensors in the same location (distance between sensor tips, <10 µm) of the ECM within the growing edge of a *S. pistillata* microcolony. ms: microsensor, **sw**: seawater, **cr**: crystals, **mt**: mesentery (**A**) Inverted brightfield image at the start of measurement with the sensor tips in the ECM. (**B**) Inverted brightfield image approximately seven minutes after start of the measurement showing retraction of the growing edge and mesentery activity.

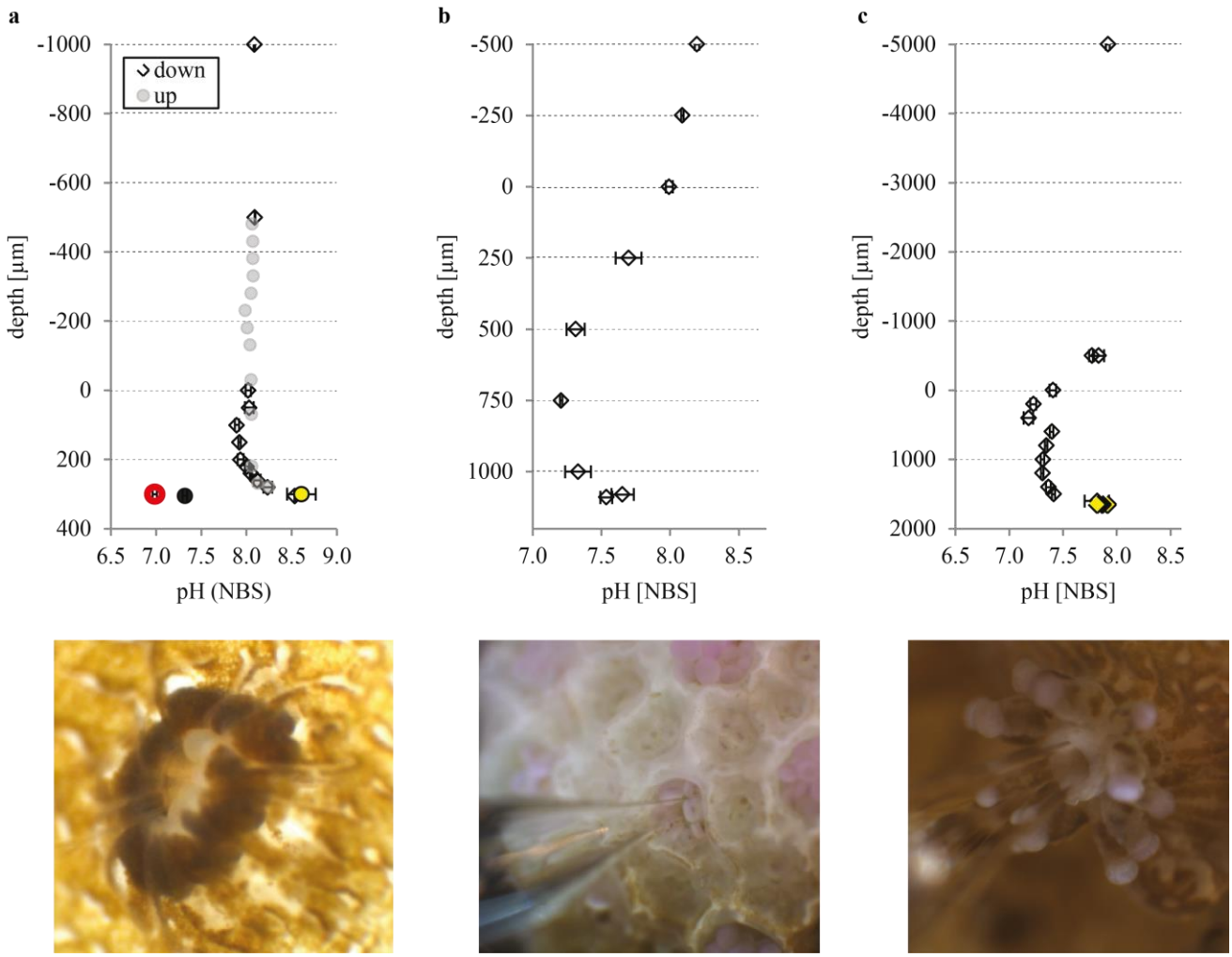

Fig. S2. pH profiles measured in the polyps of different microcolonies of *S. pistillata* by entering a pH LIX microsensor through the polyp mouth (≈0 µm). Light measurements were conducted at illumination intensities of 200 µmol photons m^{-2} s^{-1}. Pictures below the graphs illustrate the individuals measured. (**A**) Profile measured within a contracted polyp; yellow circle indicates value at the skeleton in the light; black circle gives the value at the skeleton in the dark (10 minutes dark conditions); red open circle indicates value at the skeleton after addition of DCMU to inhibit photosynthesis after the light/dark/light switch. (**B**) pH profile through the polyp of a coral apex without zooxanthellae at the coral skeleton. Yellow and black circles indicate light and dark switches as in (A), (**C**) Profile in relaxed polyp under constant illumination that did not contract over the entire period of measurement.

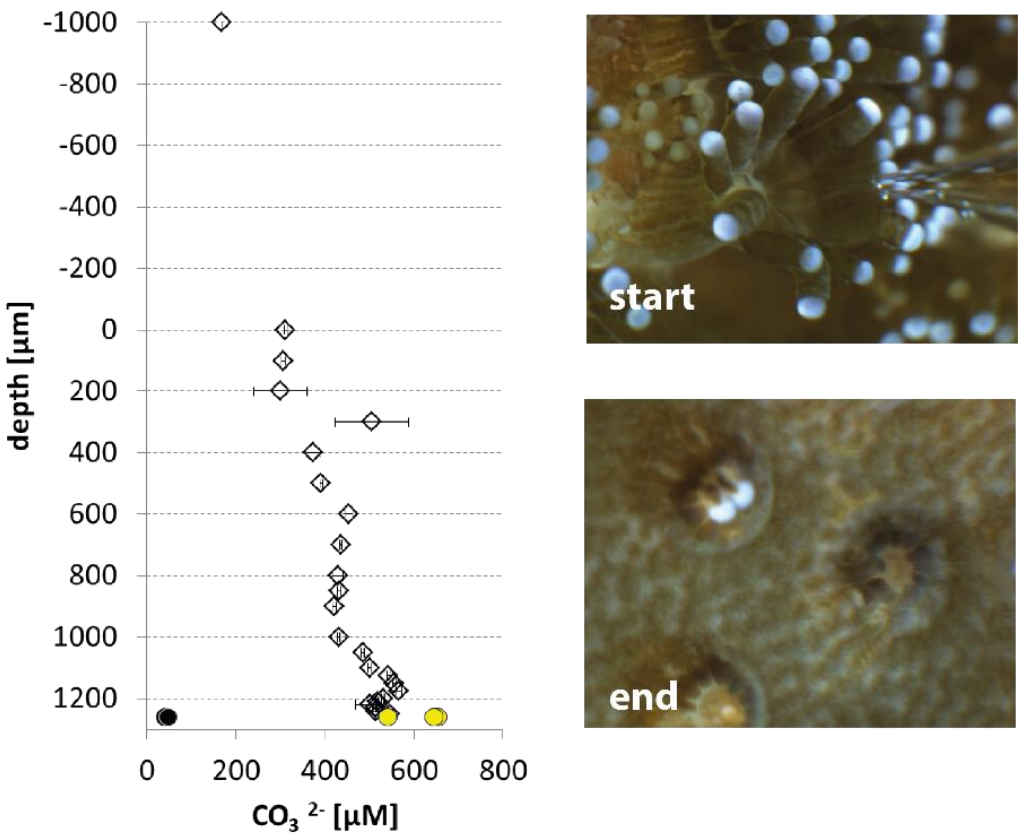

Fig. S3. Carbonate depth profile measured by entering a CO_3^{2-} LIX microsensor through the polyp mouth (at ~200 µm) of a *S. pistillata* microcolony. Measurements were conducted at illumination intensities of 200 µmol photons m^{-2} s^{-1}. Once the skeleton was reached, two light dark cycles of 10 minute intervals were applied before the sensor was withdrawn. Yellow circles indicate values at the skeleton in the light; black circles indicate values at the skeleton in the dark. Pictures at the right demonstrate the condition of the polyp at the start (relaxed) and end (contracted) of the measurement.

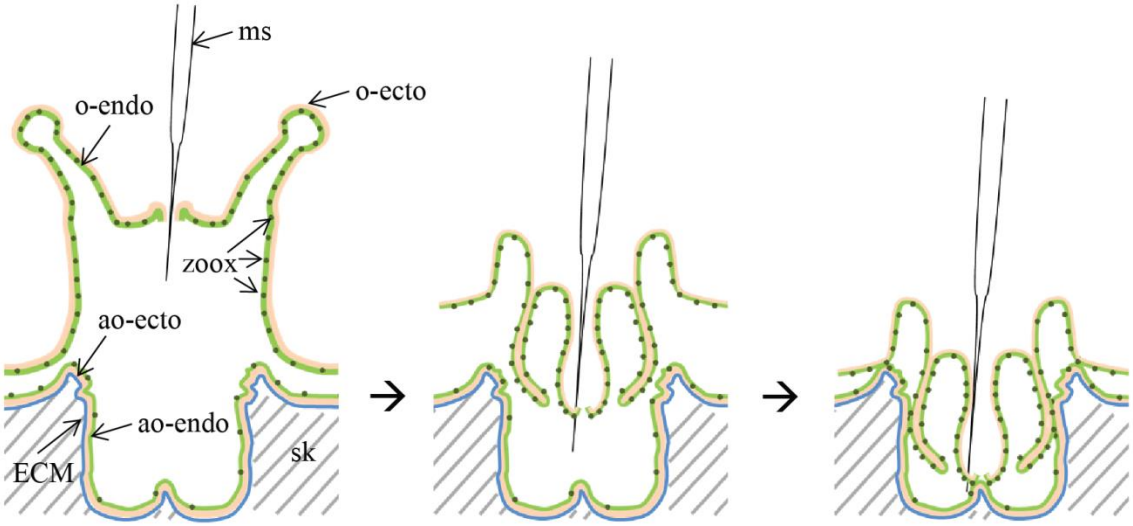

Fig. S4. Retraction of the coral polyp upon microsensor insertion. Simplified schematic overview of a coral polyp retracting upon insertion of the microsensor through the polyp mouth as observed in almost all our microsensor measurements on polyps of *S. pistillata*. The stepwise contraction of the coral polyp suggests a strong local increase of zooxanthellae density within the polyp which we propose results in a microenvironment where photosynthesis and respiration have a strong influence on chemistry at the site of the microelectrode measurement. **Orange line**: ectoderm, **green line**: endoderm, **dark green dots**: zooxanthellae, **blue line**: extracellular calcifying medium (ECM), **o-ecto**: oral ectoderm, **o-endo**: oral endoderm, **ao-ecto**: aboral ectoderm, **ao-endo**: aboral endoderm, **zoox**: zooxanthellae, **ms**: microsensor, **sk**: skeleton.

Note S1. Derivation of Eq. 1 to calculate DIC.

$K_1 = [H^+]\,[HCO_3\text{-}]/\,[CO_2]$ (a)*

$K_2 = [H^+]\,[CO_3^{2-}]/\,[HCO_3^-]$ (b)*

$DIC = [CO_3^{2-}] + [HCO_3^-] + [CO_2]$ (c)

1. Rearrange equation (a) and solve for $[HCO_3\text{-}]$

$K_1 = [H^+]\,[HCO_3^-]/\,[CO_2]$

→ $K_1\,[CO_2]/\,[H^+] = [HCO_3\text{-}]$

2. Substitute [HCO3-] in equation (b) with rearranged equation (a)

$K_2 = [H^+]\,[CO_3^{2-}]/\,[HCO_3^-]$

➔ $K_2 = [H^+]\,[CO_3^{2-}]/(K_1\,[CO_2]/\,[H^+])$

$= [H^+]^2\,[CO_3^{2-}]/K_1[CO_2]$

Solve this equation for $[CO_2]$

➔ $[CO_2] = [H^+]^2\,[CO_3^{2-}]/K_1K_2$

3. Substitute $[HCO_3^-]$ in equation (c) with rearranged equation (a) and $[CO_2]$ in equation (c) with rearranged equation (b).

$DIC = [CO_3^{2-}] + [HCO_3^-] + [CO_2]$

➔ $DIC = [\,CO_3^{2-}] + (K_1\,[CO_2]/\,[H^+]) + ([H^+]^2\,[CO_3^{2-}]/K_1K_2)$

➔ $DIC = [\,CO_3^{2-}] + (K_1\,([H^+]^2\,[CO_3^{2-}]/K_1K_2)/\,[H^+]) + ([H^+]^2\,[CO_3^{2-}]/K_1K_2)$

➔ K_1 and H^+ in second term cancel out

➔ $DIC = [\,CO_3^{2-}] + ([H^+]\,[CO_3^{2-}]/K_2) + ([H^+]^2\,[CO_3^{2-}]/K_1K_2)$

➔ factorize $[\,CO_3^{2-}]$

➔ $\underline{DIC = [\,CO_3^{2-}]\,(1+ ([H^+]/K_2) + ([H^+]^2/K_1K_2))}$ (1)

* Millero et al 2006 (*52*)

$[H^+]=10^{-pH}$ and $K=10^{-pK}$

Note S2. Calculation of the compound SD for DIC and Ω_{arag}.

To compute the **compound standard deviation σ_{Ω} for Ω_{arag}** defined as $\Omega_{arag} = \frac{[Ca^{2+}][CO_3^{2-}]}{K_{sp}}$, we consider that the values of $[CO_3^{2-}]$ and $[Ca^{2+}]$ are statistically independent random variables. A direct calculation gives thus the expression

$$\sigma_{\Omega} = \frac{\sqrt{\sigma_{CO_3}^2\sigma_{Ca}^2+\sigma_{CO_3}^2\mu_{Ca}^2+\mu_{CO_3}^2\sigma_{Ca}^2}}{K_{sp}} \times 10^{-7} \quad (3)$$

where

μ_{CO_3}= mean value of $[CO_3^{2-}]$,

μ_{Ca}= mean value $[Ca^{2+}]$,

σ_{CO_3}= standard deviation of parameter $[CO_3^{2-}]$,

σ_{Ca} = standard deviation of parameter $[Ca^{2+}]$, and

K_{sp} = solubility constant for aragonite at salinity 38 and 25°C as derived from Mucci (*53*).

The calculation for the **compound standard deviation $\sigma_{\mathbf{DIC}}$ of DIC** which is defined as $DIC = [CO_3^{2-}]\left(1 + \frac{[H^+]}{K_2} + \frac{[H^+]^2}{K_1K_2}\right)$ requires the extra (but reasonable) assumption that within the range of our measurement, the values for $[H^+]$ can be described as a Gaussian distribution. This is required in order to have an estimate of the contribution of the squared term $[H^+]^2$ to the standard deviation of the DIC.

Under such assumptions, a direct calculation shows that the mean (μ_z) and standard deviation (σ_z) of the term $z = \left(1 + \frac{x}{K_2} + \frac{x^2}{K_1K_2}\right)$ equals

$$\mu_z = \left(1 + \frac{\mu_x}{K_2} + \frac{\mu_x^2+\sigma_x^2}{K_1K_2}\right) \text{ and } \sigma_z = \left(\frac{\sigma_x}{K_1K_2}\right)\sqrt{((K_1 + 2\mu_x)^2 + 2\sigma_x^2)}$$

Combining these expressions with the formulas for the mean and standard deviation of the product of independent variables, we obtain the final result for DIC with

$$\mu_{DIC} = \mu_{CO_3}\left(1 + \frac{\mu_{H^+}}{K_2} + \frac{\mu_{H^+}^2 + \sigma_{H^+}^2}{K_1 K_2}\right)$$

$\sigma_{DIC}^2 = \left(\frac{\sigma_{H^+}}{K_1 K_2}\right)^2 \left((K_1 + 2\mu_{H^+})^2 + 2\sigma_{H^+}^2\right)\left(\mu_{CO_3}^2 + \sigma_{CO_3}^2\right) + \sigma_{CO_3}^2\left(1 + \frac{\mu_{H^+}}{K_2} + \frac{\mu_{H^+}^2 + \sigma_{H^+}^2}{K_1 K_2}\right)$, thus

$$\sigma_{DIC} = \sqrt{\left(\frac{\sigma_{H^+}}{K_1 K_2}\right)^2 \left((K_1 + 2\mu_{H^+})^2 + 2\sigma_{H^+}^2\right)\left(\mu_{CO_3}^2 + \sigma_{CO_3}^2\right) + \sigma_{CO_3}^2\left(1 + \frac{\mu_{H^+}}{K_2} + \frac{\mu_{H^+}^2 + \sigma_{H^+}^2}{K_1 K_2}\right)} \quad (4)$$

where K_1 and K_2 are the dissociation constants for carbonic acid in seawater at salinity 38 and 25°C, respectively, as derived from Millero et al. (*52*).